Studying the Effect of Rock Shape on Brittle Fracture Pattern Using a Mesh-free Method SPH

Rajarshi Das and Paul W. Cleary

***Abstract*— Numerical modelling can assist in understanding and predicting complex fracture processes. Smoothed Particle Hydrodynamics (SPH) is a particle based Lagrangian method which is particularly suited to the analysis of fracture due to its capacity to model large deformation and to track free surfaces generated. A damage model is used to predict the fracture of elastic solids. The damage parameter represents the volume averaged micro-fracture of the volume of material represented by an SPH particle. Evolution of damage is predicted using the strain history of each particle. Damage inhibits the transmission of tensile stress between particles, and once it reaches unity, it is unable to transmit tensile stress, resulting in a macro-crack. Connected macro-cracks lead to complete fragmentation. In this paper we explore the ability of an SPH based damage model to predict brittle fracture of rocks during impact. Rock shape is found to have considerable influence on the fracture process, the fragment sizes, the energy dissipation during impact, and the post-fracture motion of the fragments.**

***Index Terms*— damage, dynamic fracture, impact, SPH.**

I. INTRODUCTION

Fracture and fragmentation are governed by multiple physical processes involving different time and length scales. The sources of fracture are micro and macro voids, micro-structural defects, and initial flaws. Numerical fracture models can potentially predict both small and large scale fracturing events, ranging from breakage in mills [1] to the formation of impact craters [2]. The prediction of fracture characteristics during impact and shock wave loading and the properties of the resulting fragments provide key inputs for controlled blasts in mines [3]. Modelling breakage in granular flows is useful in optimising the design and setting operating parameters in mills to enhance mill efficiency and achieve desired product quality [1]. Furthermore, the assessment of damage initiation and progression can be rapidly and easily performed for a wide range of problem parameters, such as geometry, loading, initial defect characteristics and distribution, which are beyond the scope of experiments to explore. Effective damage modelling techniques in conjunction with efficient numerical methods have strong potential for increasing our understanding of fundamentals of breakage and for providing practical tools that can be used for equipment and structural design.

Manuscript received March 27, 2008.

R. Das is with CSIRO Mathematical and Information Sciences, Private Bag 33, Clayton, Victoria 3168, Australia (phone: 61-3-9545-8099; fax: 61-3-9545-8080; e-mail: raj.das@csiro.au).

P.W. Cleary is with CSIRO Mathematical and Information Sciences, Private Bag 33, Clayton, Victoria 3168, Australia (e-mail: paul.cleary@csiro.au).

Here we explore the potential of a particle based method called Smoothed Particle Hydrodynamics (SPH) to predict brittle failure of rocks during impact. SPH is a mesh-free numerical method which is used to obtain solutions to systems of partial differential equations. The problem geometry is discretised into 'particles' that represent specific material volumes. This method has been traditionally applied for modelling fluid flows [4,5]. In recent years, there has been a growing interest in applying SPH to a wide variety of solid mechanics problems [6-8].

SPH is preferred over traditional mesh-based techniques (e.g. FEM and BEM) for fracture prediction problems for several reasons. One primary advantage of SPH for fracture is that it does not have any underlying grid structure representing the problem geometry and so avoids the inaccuracies and instabilities associated with maintaining the integrity and quality of the mesh during large deformation. The mesh-free nature of SPH makes it ideally suited to modelling processes that involve extreme deformations and discontinuities, such as fracture and fragmentation and a broad range of geomechanics problems. Its grid-free nature enables the fracturing process and the associated change in structural configuration to be naturally handled without the need to re-mesh.

SPH is a Lagrangian method which is able to follow high speed motion without the need to include any explicit advection, and is therefore less diffusive. In general, fracturing is driven by the stress-strain history experienced by the material. Traditional Eulerian methods have difficulties in tracking the stress-strain history on a node by node basis and in predicting the evolution of damage in the specimen. The history tracking ability of SPH provides a natural framework enabling the prediction of damage initiation and crack propagation. The dynamics of damage evolution is then able to be explicitly included in the analysis.

II. DAMAGE MODELLING

Dynamic fracture is a complex phenomenon that involves the interaction between inherent or generated defects (flaws) and transient stress waves propagating within the material. The key issues in numerical modelling of damage are:

- Representing inherent initial defects in a material,
- Characterising the level of fracture at a specific location in a material,
- Representing damage growth leading to fracture.

We extend the SPH formulation for elastic solid deformation given in [6] by combining it with a continuum damage model to simulate brittle fracture. We use a modified form of the Grady and Kipp damage model [9] for the prediction of rock damage based on the local strain history and flaw distribution. A scalar damage parameter D is used to characterise the volume averaged micro-fracture of the material represented by each SPH particle in the same way as used in [9]. The damage parameter inhibits the transmission of tensile stress between particles and it evolves based on the strain history of each particle. The damage parameter lies between 0 and 1. Material with $D = 0$ is undamaged and is able to transmit the full tensile load, whereas material with $D = 1$ is fully damaged and cannot transmit any tensile load, thus creating a partial crack. Contiguous cracked material across a body leads to fragmentation. This type of model has been applied to the fracture studies of oil shale using a finite difference framework, and showed good agreement with the experimental data [10].

An approximate differential form of the Grady-Kipp damage evolution model for $D(t)$ (from [9]) is:

$$\frac{dD^{1/3}}{dt} = \frac{(m+3)}{3}\alpha^{1/3}\varepsilon^{m/3} \tag{1}$$

where ε is the tensile strain and α is a material constant determined by two material fracture parameters k and m, and the constant crack growth speed C_g:

$$\alpha = \frac{8\pi C_g^3 k}{(m+1)(m+2)(m+3)} \tag{2}$$

The original Grady-Kipp model is valid only for one dimensional plain strain problems. For use in two or three-dimensions, the full stress-strain field needs to be reduced to the one-dimensional analysis framework outlined in [9]. One proposed method replaces the longitudinal strain by the volumetric strain (average of the three longitudinal strain components) [11]. This poses difficulties when some of the longitudinal strain components are compressive and some are tensile, and their magnitudes are such that the resulting volume strain is compressive. In this case, no damage evolution will occur under a compressive strain according to this damage model, but in reality damage accumulation should take place due to the tensile component(s) of the strain tensor. To avoid this problem, Melosh *et al*. [12] introduced an effective tensile strain given by:

$$\varepsilon = \sigma_{\max} / \left(K + \frac{4}{3}G \right) \tag{3}$$

where σ_{max} is the maximum positive principal stress, and K and G are the bulk modulus and the shear modulus of the material. Damage accumulates when the effective strain exceeds a threshold $\varepsilon_{\min} = (Vk)^{-1/m}$, where V is the SPH particle volume. This effective strain is used in the evolution eq. (1) to predict the damage state of the material. So for damage evolution in SPH we use the combination of the differential version of the Grady-Kipp model (eq. 1) and the effective tensile strain (eq. 3).

The method of application of the damage to modify the momentum equation is not clear cut. A common approach has been to scale all components of the stress tensor by $(1 – D)$ [9]. This equally modifies both the compressive and tensile normal stresses, as well as shear stresses. However, the compressive stress components should not be reduced by the damage, because the material in a damaged region remains capable of transmitting forces under compression. It is only the tensile force transmission between adjacent particles that should be reduced. Another approach, proposed by Monaghan [7], is to scale all components of the deviatoric stress tensor by the damage, but to only scale the negative (tensile) pressure. Such approaches are based on ad hoc choices of which stress components the damage is applied to. A more complete approach is to rotate the total stress tensor into its principal co-ordinate frame where the tensile stress is best identified and then to scale only the tensile components of the principle stresses. These are rotated back to the world co-ordinate frame to give the post-damage stresses used in the stress evolution and momentum equations.

III. Brittle fracture during impact

Dynamic fracture of a brittle elastic solid usually occurs in three stages termed primary, secondary and tertiary. Primary fracture is the major damage experienced in the early stages and predominantly contributes towards the catastrophic failure of a structure. Damage initiates from regions with very high stress concentrations. Cracks propagate over long distances, producing sharp fracture planes and causing a high level of damage. Secondary fracture begins when additional damage or cracks are generated from either the primary fracture planes or from other highly damaged regions. These cracks propagate over shorter distances and produce smaller fragments or localised debris than those generated by primary fracturing. During secondary fracture the fragments remain within the space of the original structure. Tertiary fracture is localised fracture that occurs when fragments/debris fly off and collide with other fragments.

Changes in fracture pattern during impact on a rigid surface with change in the rock shape are investigated using three idealised rock forms (circular, annular and square). In all cases, the same sandstone is used. It has a bulk modulus of 12.2 GPa, a shear modulus of 2.67 GPa and a density of 2300 kg/m^3. The Weibull damage parameters k and m (in eq. 2) are 1.0×10^{22} and 9.0 respectively (taken from [12]). The same impact velocity of 100 m/s is used for all cases. The left and right columns of Figs. 1-3 are coloured by the von Mises stress and damage respectively. For the stress, the colour variation (blue-red) corresponds to a stress range of 0 to 5 GPa and for damage the range is 0 to 1. Time is measured from the instant of first contact of the rock with the surface.

A. Circular shape

Fig. 1 shows the impact of a circular rock on a rigid surface. It has a diameter of 100 mm and used 2,029 SPH particles. As the rock compresses vertically, high tensile stresses are generated in its centre. This extends along four radially outward paths, leading to the generation of damage radiating from the center of the disk (Fig. 1a). Two of the branches are close together and directed upwards, and the other two lie close together and point down. The damage paths grow rapidly and asymmetrically. The high stress between the centre and the contact point causes the bottom damage paths to grow faster than the top ones. At 0.11 ms the length of the bottom damage paths is about twice that of the top ones.

The narrow high stress zones rapidly reach the periphery of the rock and damage continues to propagate along these stress paths (Fig. 1b). These form the primary fracture planes which are inclined at angles of approximately 20^0 to the vertical. Two highly damaged regions are generated on the left and right of the upper fracture planes. The region between the lower fracture planes is also highly damaged due to the high impact stresses. High damage is also produced around the circumference of the rock. The primary fractures create two large fragments on the sides and a small fragment at the top. The very high stresses between the center of the disc and the contact point generate a cloud of debris composed of pulverised fine materials (Fig. 1c).

The high stresses near the top of the two large fragments cause secondary fracture, which results in two small fragments being created from their tops. Fig. 1d shows the fragments separating. We observe very little tertiary fracture of these fragments. In this case, the tertiary fracture mainly occurs by progressive delamination from the surfaces of the flying fragments. The fragments move primarily vertically with varying speeds. The two large fragments rotate slightly in opposite directions while they move apart.

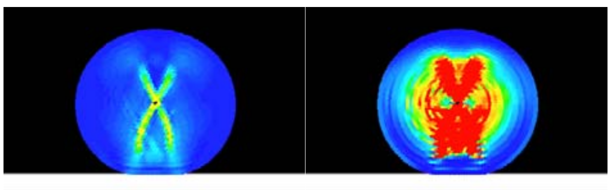

a) t = 0.11 ms

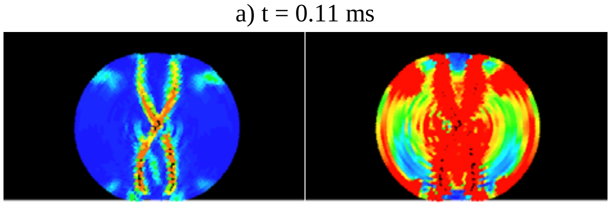

b) t = 0.16 ms

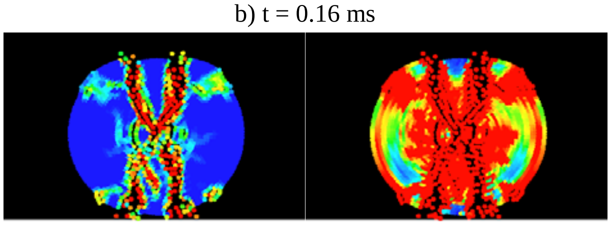

c) t = 0.31 ms

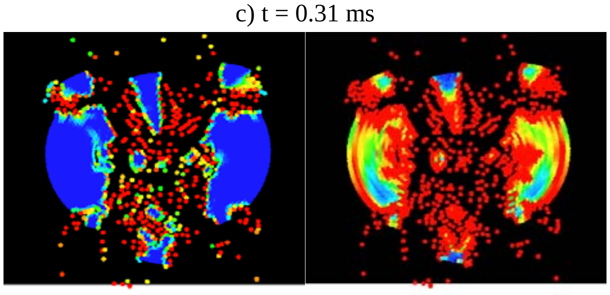

d) t = 0.86 ms

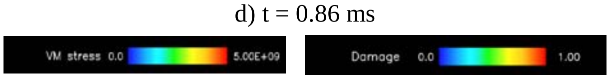

Fig. 1: Brittle fracture of a circular rock, coloured (left) by von Mises stress and (right) damage.

B. Annular shape

Fig. 2 shows the brittle fracture of an annular rock when impacting a rigid plate. The outer and inner radii of the rock are 100 and 50 mm respectively, and the SPH model has 1,664 particles. Fig. 2a shows the stress and damage as the rock first comes in contact with the rigid surface. The high normal contact force generates high stresses at the bottom of the rock. This pushes up the central section and initiates fracture at the bottom of the inner annular surface. The compression generates lateral tension and the rock bulges sidewise. The resulting high stresses at the lower left and right sides cause damage originating from the outer surface of the rock. This is different to the fracture behaviour of the circular rock where the damage first appeared at the centre.

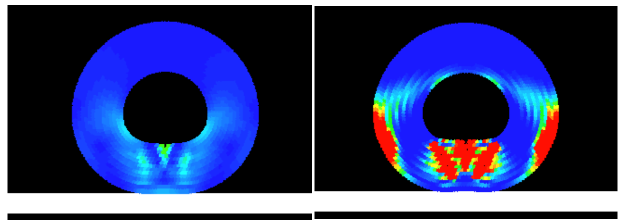

a) t = 0.06 ms

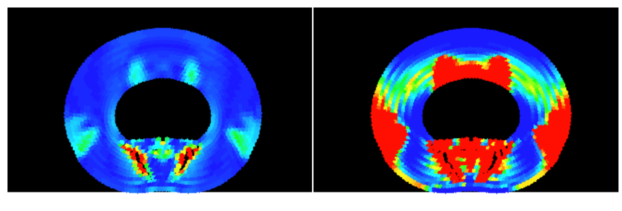

b) t = 0.11 ms

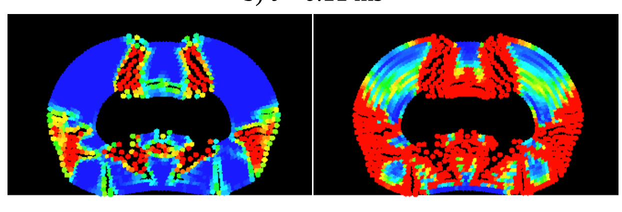

c) t = 0.21 ms

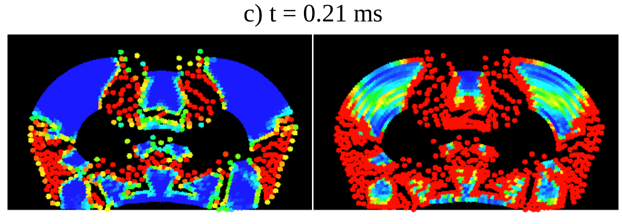

d) t = 0.31 ms

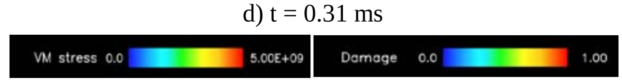

Fig. 2: Brittle fracture of an annular rock, coloured (left) by von Mises stress and (right) damage.

The higher stresses at the bottom of the inner surface lead to radial propagation of damage creating three fracture planes emanating from the lower inner surface at 0.11 ms (Fig. 2b). The central fracture plane is shorter, whilst the relatively longer ones on the either side are inclined about 45^0 towards the point of contact with the rigid surface. The high stress regions in the lower outer and upper inner surfaces cause further damage. The damage on the outer surface is distributed over a wide region and moves inward. A damaged zone is also generated at the top of the inner surface. By 0.21 ms the damage at the lower inner surface propagates further

ISBN:978-988-17012-3-7

down and the damage on the outer sides approaches close to the inner surface (Fig. 2c). At the top inner surface, the damage extends along two nearly vertical fracture planes. This is accompanied by the creation of a U-shaped fracture zone. From the outer surface at the bottom, two damage paths start growing vertically. These grow rapidly and the primary fracture occurs along both horizontal and vertical planes (Fig. 2d). Two large fragments are produced on the sides. A small fragment at the top and a number of small fragments at the bottom are also created. These fragments are surrounded by pulverised fine material. The high stresses on the lower left and right sides lead to secondary fracture that produces a debris cloud. The two large side fragments and a number of smaller fragments move predominantly in the horizontal direction. The small fragment on the top moves vertically down and collides with the debris cloud travelling upwards. This leads to tertiary fracture creating additional smaller fragments and fine particles.

C. Square shape

Fig. 3 shows the impact of a square rock on a rigid plate. The rock has sides of 100 mm and consists of 2,514 SPH particles. The vertex of the rock that collides with the surface is subjected to a high stress due to the sharp geometry. High tensile stresses are also generated in the middle of the rock. Damage is simultaneously initiated from the left side slightly above the contact point and the centre of the specimen (Fig. 3a). The damaged zone is quite large in the middle, whereas it is small and localised above the contact point at 0.17 ms. The highly stressed central region generates damage that grows rapidly in both directions from the centre along the diagonal from the contact vertex (Fig. 3b). The damage originating near the contact vertex grows relatively slowly towards the diagonal of the square. The two damage paths merge close to the vertex leading to primary fracture along the diagonal.

High stresses around the primary fracture plane cause a wide band of damage to develop on both sides of the diagonal which grows towards the interior (Fig. 3c). The primary fracture plane starts near the contact point, passes through the centre and extends up to a point P, located halfway between the center and the opposite corner. From here, the damage grows in two branches, leading to secondary fracture up to the top and right edges (Fig. 3d). The narrow high stress paths correspond to the primary and secondary fracture planes. Numerous very short cracks emanate from the top and bottom edges of the rock. The primary fracture divides the rock diagonally into two large fragments, and the subsequent secondary fractures produce two smaller fragments near the bottom left and top right corners (Fig. 3e). Unlike the primary fracture along the vertical and horizontal planes observed for the circular and annular rocks, here the fracture occurs along an inclined plane. The short cracks at the top and bottom surfaces lead to some delamination (tertiary fracture) of these surfaces. The large fragments at the top and bottom move vertically rotating slightly clockwise. The two smaller fragments travel horizontally (Fig. 3f). The fragments undergo considerable tertiary fracture while travelling apart.

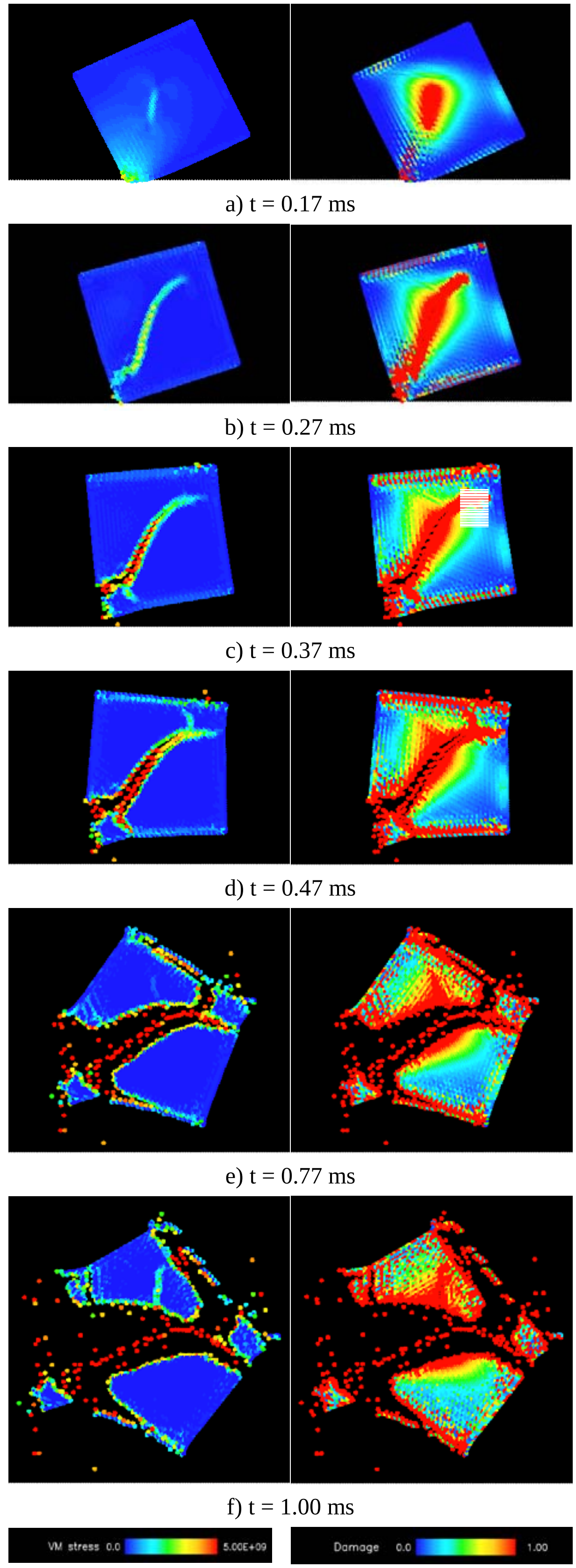

Fig. 3: Brittle fracture of a square rock, coloured (left) by von Mises stress and (right) damage.

D. Comparison of damage development

Fig. 4 shows the variation of the average damage in the material during the three impacts. There are three distinct

ISBN:978-988-17012-3-7

regions; 1) the initial rapid rise up to point P which represents the primary and subsequent secondary fracturing of the rocks, 2) the lower damage rate from point P to Q represents the small scale tertiary breakage, and 3) the final constant damage level once fracturing is complete. For the circular rock there is very little tertiary damage as indicated by the lack of change between P_c and Q_c. For the annular rock, the primary and secondary damage finishes earlier and at a lower level of damage of 0.6 compared to the circular case where it was 0.7. Tertiary damage is observed for the annular rock with the damage level increasing to 0.8. The square rock experiences the lowest level of damage of 0.4 during the primary and secondary fracture (up to P_s), and this occurs much more slowly than for the previous shapes (around twice as long). This case also experiences the highest level of tertiary fracture leading to a final damage of 0.82. Approximately half of the total damage occurs during the tertiary fracture for this case. The final average damage to the rock is very similar for the annular and square shapes and it is higher than that for the circular rock. The different load paths lead to quite different distributions of damage and so quite different fragmentation and debris patterns.

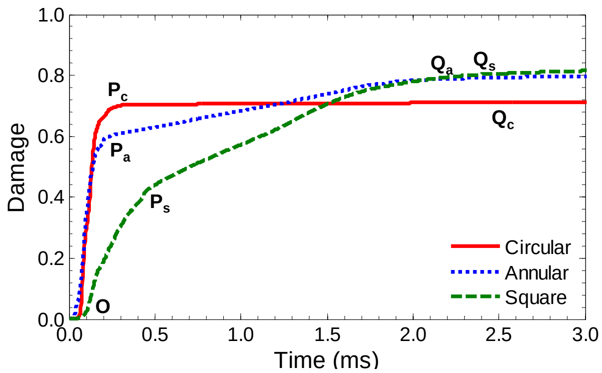

Fig. 4: Variation of average damage with time since commencement of the collisions for different rock shapes.

E. Velocity distribution of the fragments

Fig. 5 shows the distribution of the fragments at 0.86 ms with the particles coloured by their velocity (dark blue being stationary and red being 220 m/s). The velocity and size of the fragments are strongly dependent on the initial shape of the rock. For the circular case, two large and a number of relatively smaller fragments are produced. A moderate level of debris is also produced between these fragments. The fragments move predominantly vertically upwards. The upper fragments and debris particles have a higher velocity (around 90 m/s) than the lower ones. For the annular rock, a number of large and small fragments are also created. Some debris particles move at speeds as high as 160 m/s. The fragments of the annular rock move primarily horizontally. The velocity of the larger upper fragments (~110 m/s) is also higher than that for the circular case. Comparatively little fine debris is produced by the square rock. The two large fragments move primarily vertically upwards, whereas the smaller ones travel horizontally. The variation in velocity within the large upper fragment indicates high strain gradients and the potential for tertiary fracture as the fragments fly off.

Fig. 6 shows the variation of kinetic energy ratio of the rocks during impacts. Upon contact with the rigid surface, the rocks undergo elastic compression and then brittle fracture. Primary and secondary fractures occur in a short time after the impact. The initial kinetic energy of the rock is converted into, a) the elastic energy stored in the rock, b) the energy dissipated in fracture, and c) the kinetic energy of the accelerated fragments.

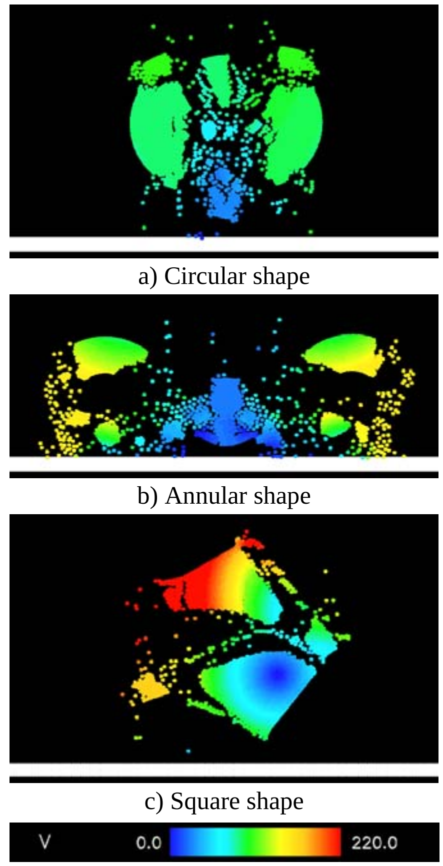

Fig. 5: Velocity distribution of the fragments for different initial shapes of the rock.

The early loss of kinetic energy (up to points labeled R) represents the total energy dissipated in fracture and stored in elastic compression. Elastic unloading of the rock transfers some energy back into kinetic energy (between points R and S). Primary and secondary fracturing has effectively ceased at points S_c and S_a for the circular and annular rocks, and thereafter the kinetic energy of the bodies (debris cloud and fragments) decreases only slightly due to tertiary fracture. For the square rock, primary and secondary fracturing occurs slowly and continues beyond point S_s. The minimum kinetic energies obtained are 6%, 48%, and 16% of the initial kinetic energies for the circular, annular, and square shapes respectively. The very low values for the first and third rocks indicate that they almost come to rest during the elastic loading and primary fracture. The annular rock fractures more rapidly before it has slowed significantly so the fragments retain a higher kinetic energy at the end of elastic compression compared to the other two shapes. The rapid fragmentation causes the annular rock to experience the lowest elastic compression. It stores only 14% of its initial kinetic energy as elastic strain energy, whereas the elastic energies stored by the circular and square rocks are 34% and

72% respectively. The elastic loading-unloading occurs over 0.16, 0.19, and 0.25 ms for circular, annular and square cases respectively. The kinetic energy change after this is 2%, 11%, and 9% for the three cases. This is consistent with the average damage variation in Fig. 4.

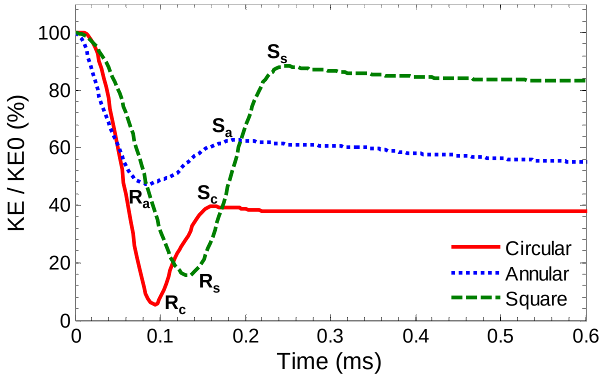

Fig. 6: Variation of the kinetic energy ratio during collision for different rock shapes.

The overall change in the kinetic energy represents the energy consumed in fracturing. The fractions of the initial kinetic energy lost during impact are 62%, 48%, and 20% for the circular, annular and square rocks respectively. The energy dissipated in fracturing is used in creating new surface area of the fragments and depends on the fracture pattern and the fragment size distribution. The larger volume of pulverised fine debris and the smaller fragments produced during the impact of the circular and annular rocks consume more energy. The coefficient of restitution, defined here as the ratio of the average post-collisional speed to the initial rock speed, is found to be around 0.79, 0.69, and 0.45 for the circular, annular, and square rocks respectively.

IV. Conclusions

SPH has been able to successfully model brittle fracture of rocks during impact with a rigid surface. It can effectively simulate the complex variation in stress and damage, and the resulting fragmentation patterns experienced during impact. The SPH solutions are sensible and demonstrate the key physical phenomena that occur in a fracturing process.

SPH appears to be well suited to modelling brittle fracture during impact. It has the advantage of being able to follow very high deformations including self-collision (beyond what is possible with the FEM and FV methods) due to the absence of any grid structure with any pre-defined connectivity. It naturally keeps track of the material free surfaces generated by fracturing, and thus allows the prediction of the propagation of damage and/or cracks. Upon fracture the motion of the fragments can be tracked naturally because of the Lagrangian nature of SPH. This enables simulation of secondary and tertiary fracture and the collision of fragments with surrounding objects. SPH can model the complex dynamic stresses associated with collision and fracture. This results from the ability of the SPH particles to automatically advect stress, strain history and micro-mechanical properties with them as they move. This potentially allows the incorporation of complex rate dependent constitutive material behaviour and direct prediction of the change in thermo-mechanical properties during fracture.

For the brittle fracture of the rocks under impact, it was found that:

- Primary fracture occurs along planes inclined at specific angles to the direction of the initial motion of the rock. They are highly dependent on the rock geometry which determines the weakest plane for a given impact stress loading. This is a typical characteristic of such impacts observed in experiments and real life failures. The primary fracture planes are vertical for the circular shape, are both vertical and horizontal for the annular shape, and are diagonal for the square shape.
- Secondary fracture and the size of the resulting fragments also depend strongly on the shape of the rocks. The circular and annular rocks undergo significant secondary fracture compared to the square one, and produce more fine debris.
- For the annular and square rocks, tertiary fracture plays an important role. It takes place over a much longer time and can cause considerable damage, as was observed for the square rock.
- The mode of fracture affects the total damage of the rocks. During primary and secondary fractures, the damage rises rapidly with the rate of rise being dependent on the rock shape. During tertiary fracture, the damage increases more slowly or remains constant for the circular rock.
- The rock shape is found to have considerable influence on the final motion of the fragments. The fragments move vertically after impart for the circular and square shapes, whereas they fly off horizontally for the annular rock.
- The fraction of the kinetic energy dissipated during fracture strongly depends on the shape of the rock with the circular and annular rocks consuming significantly more energy than the square rock.

V. References

[1] R.D. Morrison, and P.W. Cleary, "Using DEM to model ore breakage within a pilot scale sag mill," *Min. Eng.*, Vol. 17, 2004, pp. 1117-1124

[2] H.J. Melosh, and G.S. Collins, "Meteor Crater formed by low-velocity impact," Nature, Vol. 434, 2005, pp. 157.

[3] R.J. Mitchell, 1993. *Physical modelling of fracture and flow in mine backfills*. In Kingston, Ont, Can. 93. A.A. Balkema.

[4] J.J. Monaghan, "Smoothed particle hydrodynamics," *Ann. Rev. Astron. Astrophys*., Vol. 30, 1992, pp. 543-574.

[5] P.W. Cleary, M. Prakash, J. Ha, N. Stokes, and C. Scott, "Smooth particle hydrodynamics: status and future potential," *Progress in Computational Fluid Dynamics*, Vol. 7, 2007, pp. 70-90.

[6] J.P. Gray, J.J. Monaghan, and R.P. Swift, "SPH elastic dynamics," Comp. Meth. in App. Mech. and Eng., Vol. 190, 2001, pp. 6641-6662.

[7] J.P. Gray, and J.J. Monaghan, "Numerical modelling of stress fields and fracture around magma chambers," *J. Vol. Geo. Res*., Vol. 135, 2004, pp. 259– 283.

[8] P.W. Cleary, M. Prakash, and J. Ha, "Novel applications of smoothed particle hydrodynamics (SPH) in metal forming," *J. Materials Processing Technology*, Vol. 177, 2006, pp. 41-48.

[9] D.E. Grady, and M.E. Kipp, "Continuum modelling of explosive fracture in oil shale," *Int. J. Rock Mechanics and Mining Sciences & Geomech*. Abstracts, Vol. 17, 1980, pp. 147-157.

[10] D.E. Grady, M.E. Kipp, and C.S. Smith, 1980. "Explosive fracture studies on oil shale". *SPEJ, Soc. Petroleum Engineers J.* (5): 349-356.

[11] B.J. Thorne, P.J. Hommert, and B. Brown, 1990. Experimental and computational investigation of the fundamental mechanisms of catering. In 3rd Int. Symposium on Rock Fragmentation by Blasting, in Brisbane, Australia. 117-124.

[12] H.J. Melosh, E.V. Ryan, and E. Asphaug, "Dynamic fragmentation in impacts: hydrocode simulation of laboratory impacts," *J. Geophys. Res.*, Vol. 97, 1992, pp. 14735– 14759.

ISBN:978-988-17012-3-7